LIGO-xxxxxxx-xx-x	2012/07/04

GEO Squeezing Noise Budget

Kate Dooley, Hartmut Grote, Henning Vahlbruch (*alphabetical order for now*)

Draft

1   Introduction

This document serves as a summary of the current understanding of the noise budget of the GEO squeezer. It includes the following:

- overview of the GEO squeezer setup

- review of mechanisms by which the squeezing level as seen in h is affected

- description of methods and results of measurements of the optical losses and phase noise

- design and characterization of the control loops that intregrate the squeezer with the interferometer

- suggestions for future work

2   Overview of squeezing setup

A description of the GEO squeezer itself can be found in Ref. [Henning's 2010 Class. Quantum Grav. paper]. Coherent control sidebands, Faraday isolator injection point, ...

3   Reductions to potential squeezing

The amount of squeezing that can be achieved with an interferometer is a function of three primary quantities:

1. level of injected squeezing

2. optical losses (including mode-matching and alignment)

3. phase noise

Models are presented here and measurements follow in the next sections.

3.1   Injected squeezing

The level of injected squeezing is limited to the performance of the squeezer itself. The level of squeezing generated by the squeezer can be controlled during interferometer operations
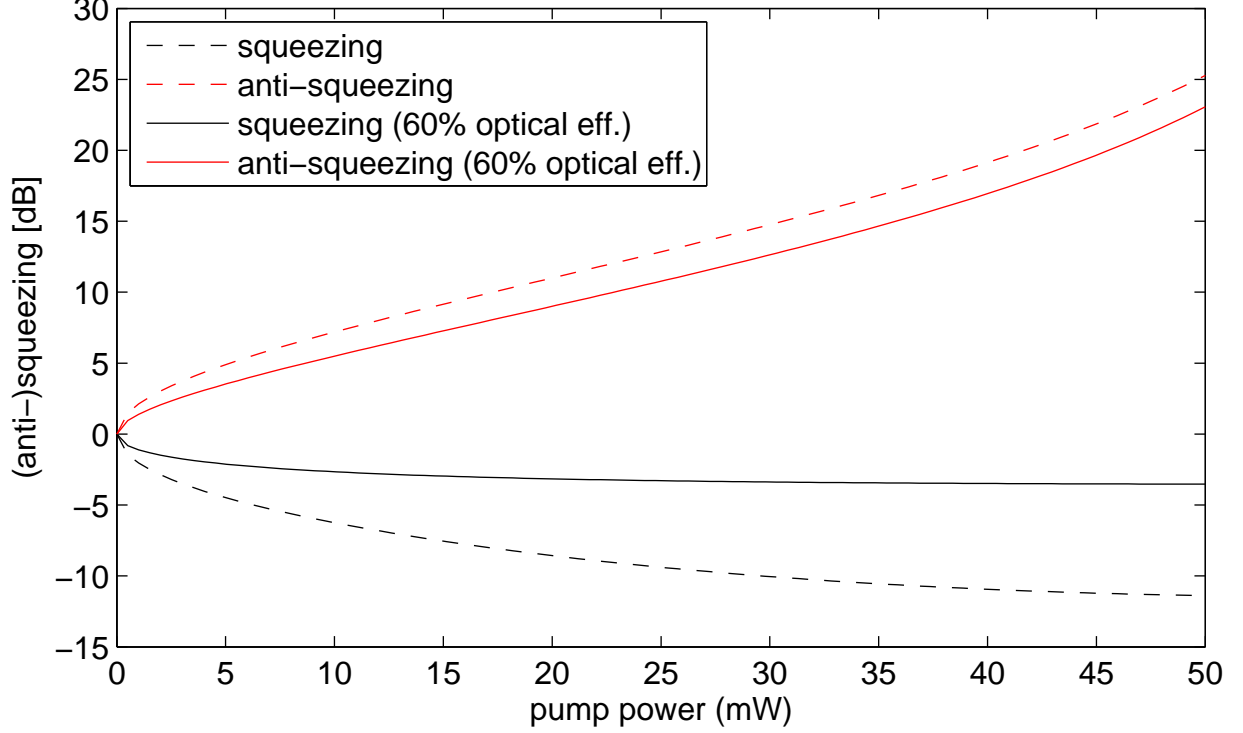
Figure 1: The amount of generated squeezing and anti-squeezing as a function of the green pump power. An example of the effect of optical losses is included by showing the equivalent curves when the optical efficiency of the squeezer path is 60%. No phase noise is included.

by changing the setpoint for the Mach-Zehnder (MZ) in the squeezing box. A PZT on one of the MZ mirrors changes the MZ length and therefore controls the amount of green light transmitted through the MZ to match the requested setpoint. This green pump field is sent directly into the OPA cavity to generate the correlated 1064 nm photons. The degree of squeezing is a non-linear function of the pump power and is plotted in Figure 1 using the GEO squeezer parameters which are found in Table 1. This shows the upper limits of our achievable squeezing level. A maximum pump power of 45 mW, or 11 dB of generated squeezing, may be used with the GEO squeezer.

Table 1: GEO squeezer parameters (see p.70, 90 Khalaidovski thesis).

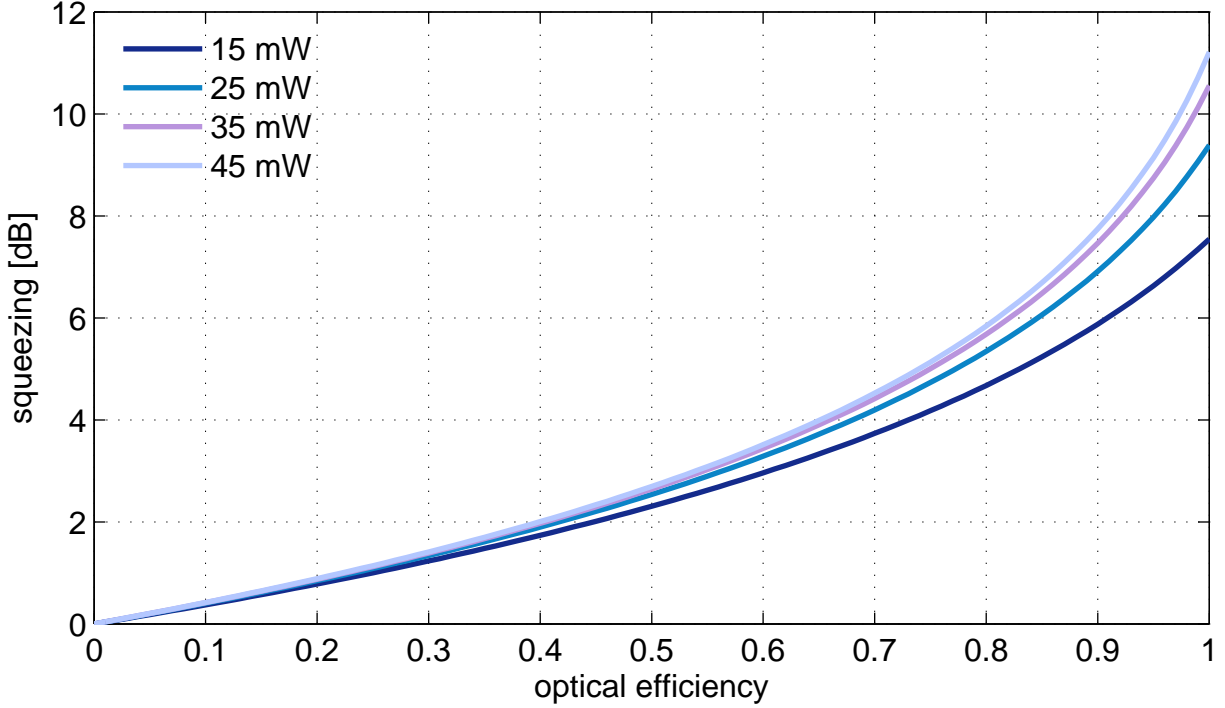|	
squeezer breadboard optical efficiency	93%
OPO output coupler transmission	8%
OPO intracavity loss	4%
OPO round-trip length	0.0186 m
frequency	5 MHz
OPO threshold power	60 mW

Figure 2: The expected amount of observed squeezing based on the green pump power and the optical efficiency of the squeezed field path. This model assumes no phase noise.

3.2 Optical losses

Any time the squeezed vacuum field experiences an optical loss, the loss is replaced by the classic vacuum field:

$$V' = VT + L \tag{1}$$

Here, V is the initial variance of the squeezed state, T the optical efficiency, and L the optical losses, where $T + L = 1$. Figure 2 shows the how the degree of squeezing is degraded as a function of optical efficiency for several different pump powers.

3.3 Phase noise

Phase noise arises when there is relative motion between the angle of the squeezing ellipse and the angle of the measurement quadrature of the interferometer. The degree of (anti-)squeezing is reduced to the following quantities for an rms phase noise of θ:

$$V'_s = V_s \cos^2\theta + V_a \sin^2\theta \tag{2}$$
$$V'_a = V_a \cos^2\theta + V_s \sin^2\theta \tag{3}$$

where V_a and V_s are the variances of the anti-squeezed and squeezed states, respectively, before including the effect of phase noise. Note that for small θ, the change in the (anti-
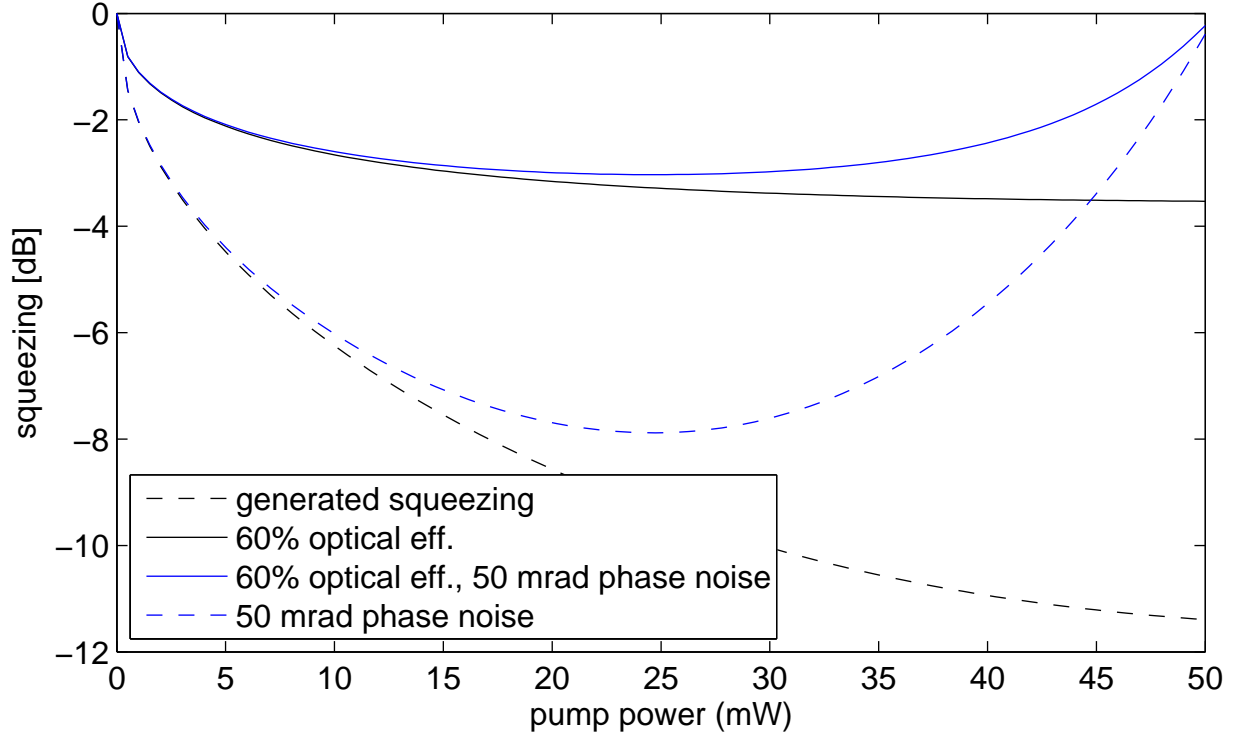
Figure 3: Generated squeezing as a function of the pump power (black dashed curve) shown in contrast with the equivalent curves that include 40% optical losses and 50 mrad phase noise. These numbers are selected for demonstration purposes only.

)squeezed states depends linearly on the degree of squeezing/anti-squeezing, respectively. Given the amount of anti-squeezing is much greater than the amount of squeezing (see Fig. 1), the squeezed state is much more significantly affected by phase noise than the anti-squeezed state. Figure 3 shows how the squeezing as a function of pump power is reduced most significantly at high pump powers (ie. where there are the highest levels of anti-squeezing). Figure 4 shows squeezing as a function of phase noise for several pump powers when the optical losses are 40%. The highest pump power of 45 mW is only beneficial if the total rms phase noise is less than 10 mrad.

4   Optical losses

Table 2 summarizes our optical loss budget for the squeezer path. We find that only 63% of the squeezed light sent into the interferometer makes it to the detection PD. With the nominal 35 mW pump power, or 10.5 dB injected squeezing, these optical losses alone reduce the maximum possible level of achieved squeezing to 3.7 dB.

The single greatest source of loss is the OMC and second is the detection PD. The OMC is known to have excessive losses due to poor AR coatings and most likely dirty mirrors and
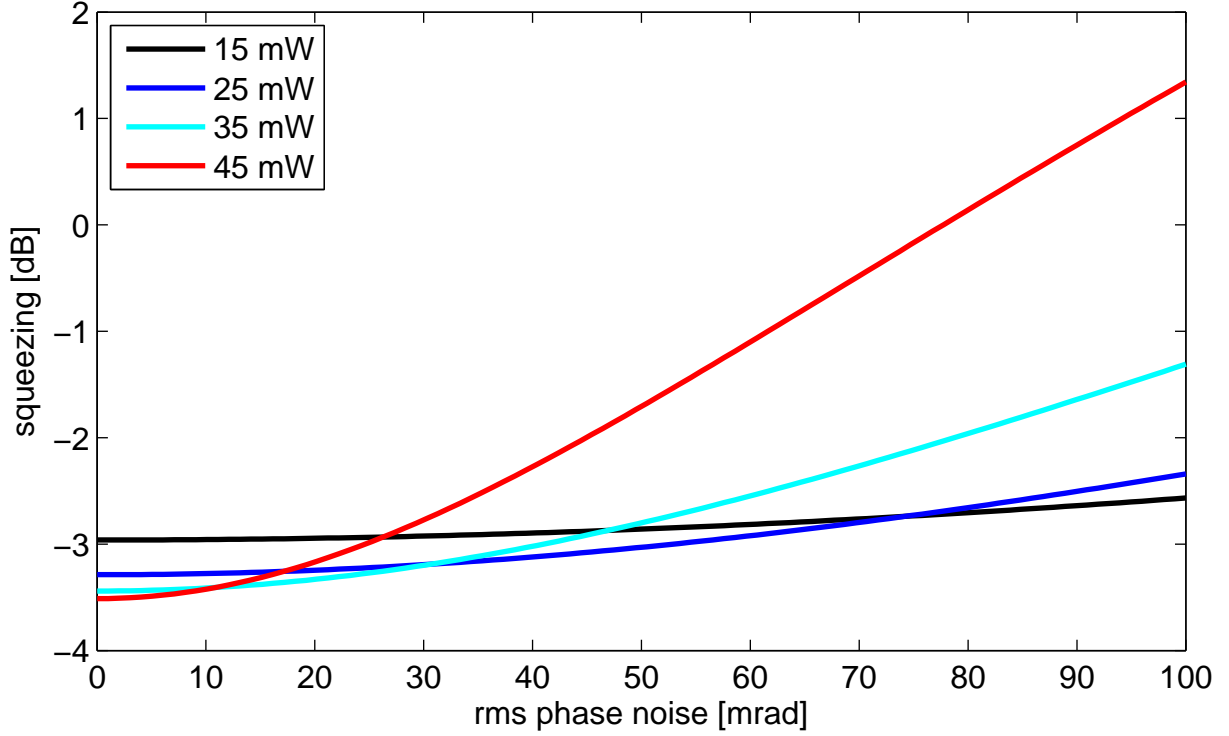
Figure 4: Squeezing as a function of phase noise for 4 different pump powers when optical losses are 40%.

Table 2: Optical losses of squeezed beam. The resulting transmission upon multiplying the optical efficiencies in series is 63%.

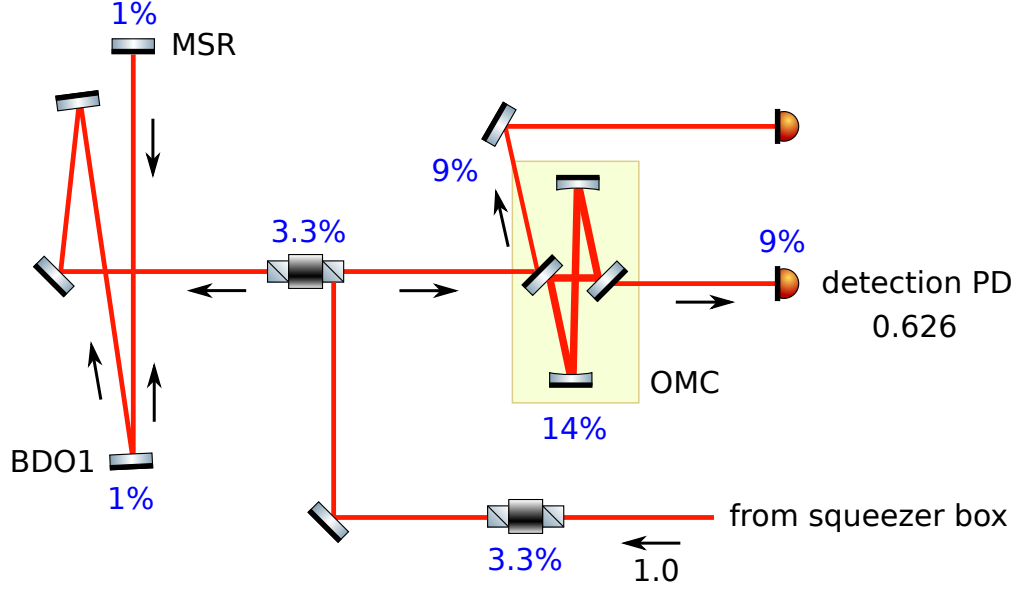| component	power loss	comment
squeezer path Faraday	3.3%	1.5%
output port Faraday	3.3% × 2	guess
BDO1 transmission	1% × 2	
SR cavity (when locked)	1%	above 1 kHz
OMC mode-matching loss	6%	
squeezer mode-matching loss	2%	
OMC AR coating loss	1%	
OMC internal losses	14%	deduced from other measurements
OMC trans PD detection loss	9%	Perkin-Elmer

Figure 5: Optical losses in the squeezer path.

can in principle be easily improved with new optics. The current Perkin-Elmer photodiode is also a high-loss component that can be replaced with a much better specimen. The polarizing beam splitters of the Faraday isolators each have approximately 1% loss and with investigation into better polarizers, may be improved. Details of short-term goals for improvement of optical efficiency are found in Section 7.

4.1 Mode-matching

The mode-matching lenses used to match the squeezed field into the OMC were selected based on a model, and then tuned in-situ. The bright alignment beam was used and the OMC scanned to look for minimizing the TEM02/20 mode. The mode-matching is approximately 98%.

4.2 Alignment

The squeezed field needs to be aligned to the carrier field at the inteferometer output port. There are several ways of generating an alignment signal, all of which use the squeezer coherent control sidebands. The true alignment signal is the beat between the carrier TEM00 and CCSB TEM01/10. However, most of the carrier light at the output port is made of higher order modes which add noise to the measurement. Because the Michelson sidebands are spatially cleaner at the output port than the carrier (and should be aligned to the carrier), they serve as a potential alignment signal candidate. A summary of the options explored for generating an alignment signal are found in Table 3.

Include plot of first results.

Table 3: Options for generating an alignment error signal.

where	what	frequency
OMC REFL QPD	CCSBs vs. MI RF SBs	300 kHz
FAR camera	CCSBs vs. carrier	15.2 MHz
FAR camera	CCSBs vs. MI RF SBs	300 kHz

5 Phase noise

The squeezing ellipse orientation must match the angle of the interferometer output field to make the best use of the squeezed field. The interferometer output field is ideally made up of only the local oscillator for the gravitational-wave signal, the dark fringe offset. However, in practice, other light is present and contributes to the shot noise at the detector. The power of squeezing is that it can reduce the shot noise of the light at the output port, no matter what it is made of. Therefore, the sum of the phase jitters of all fields must be considered. In addition, it should be pointed out that only the rms phase noise matters, not the shape of the frequency content.

5.1 Phase noise sensing and control

There are several options for how to implement a squeezer longitudinal phase servo. First, there are three choices for how to generate such an error signal. ...

Second, there are choices for how to feedback a control signal. ...

Our current setup for creating a squeezer to GEO output relative phase error signal uses the beat of the squeezer sidebands with the Michelson sidebands in reflection of the OMC which are at 15.2 MHz and 14.9 MHz, respectively. A sample error point spectrum is shown in Figure 6 and demonstrates that we measure only 5 mrad rms residual phase noise. We also inject a line at 6500 Hz to monitor the signal-to-noise of the error signal.

5.2 Noiselock

We implement a slow servo called the *noiselock loop* that serves to change the squeezing quadrature in order to maximize the strain sensitivity. The demodulation phase of the longitudinal phase error signal is dithered at 11.6 Hz and a band-limited root-mean-square of strain is then demodulated at this dither frequency and a control signal derived. A schematic of the servo is in Figure 7. The underlying causes for slow phase drift is not understood at this time. An example of how much drift we observe is shown in Figure 8.
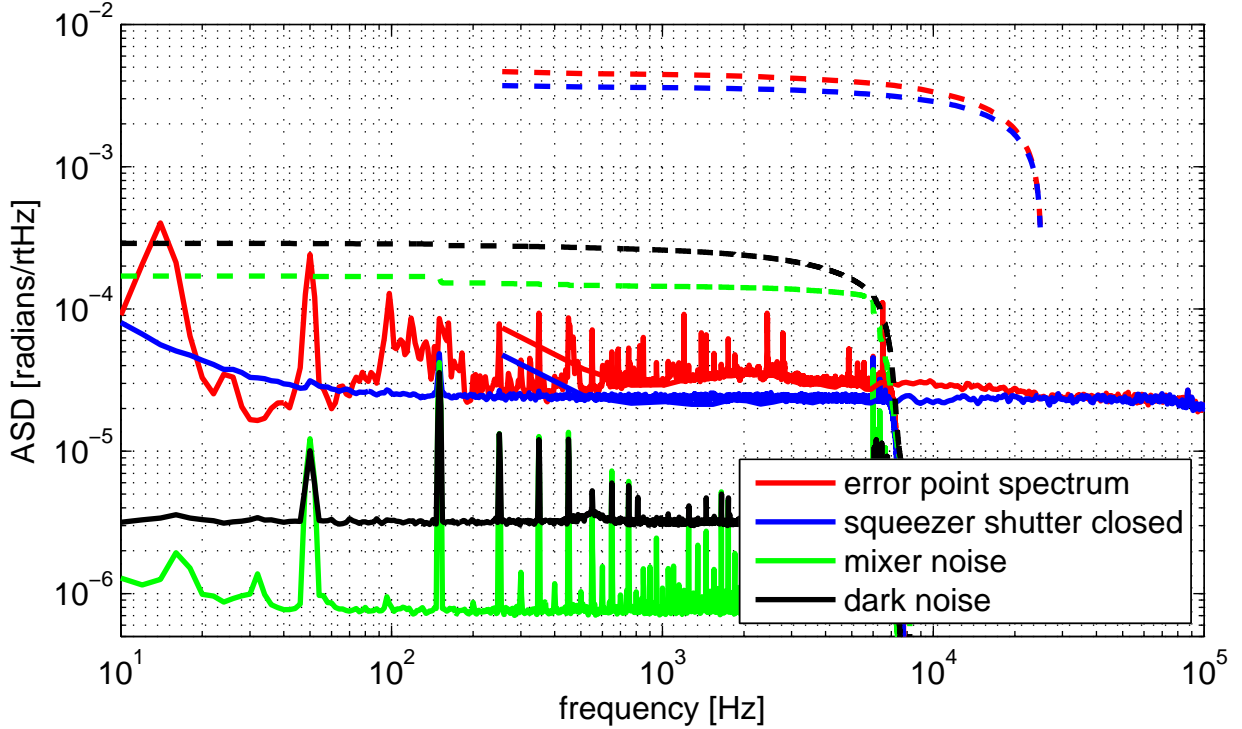
Figure 6: Calibrated squeezer phase error point (red curve), measured as the beat between the squeezer control sidebands and the RF Michelson sidebands in reflection of the OMC. This loop operates with a bandwidth of about 1 kHz and is limited by sensor/shot (blue curve) above 25 kHz. The servo is not gain-limited because the spectrum is so flat such that little to no improvement in rms noise is to be gained by increasing the gain. The residual rms phase noise is 5 mrad.
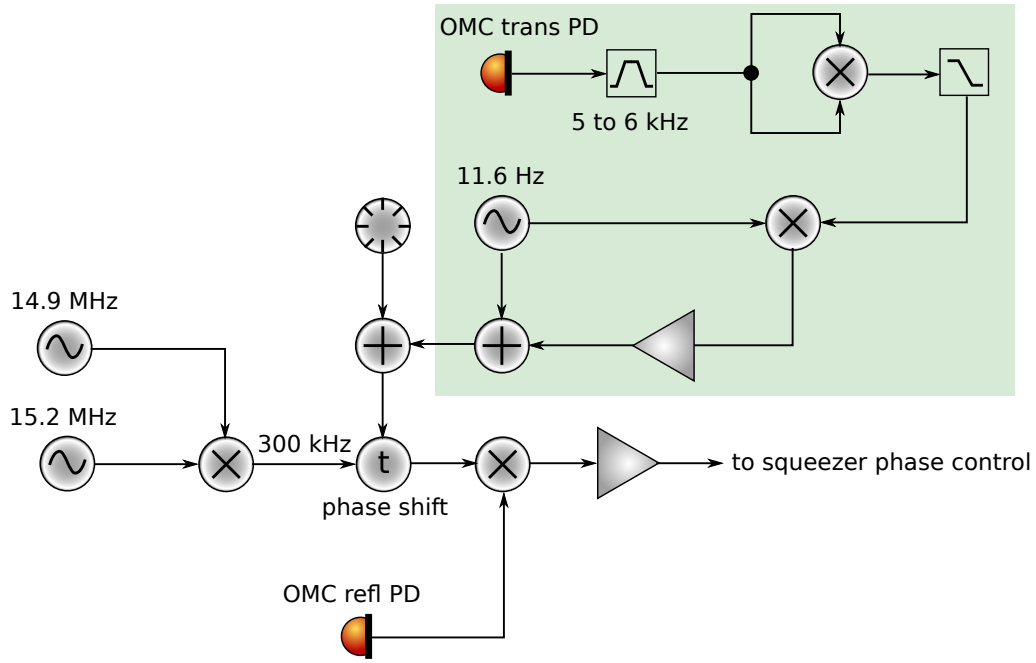
Figure 7: Schematic of the noiselock servo. The demodulation phase of the squeezing angle error signal is modulated at $f_0 = 11.6$ Hz. The band-limited rms of interferometer strain is in turn demodulated at f_0 and a derived control signal is in turn sent to the demodulation phase of the squeezing angle error signal.
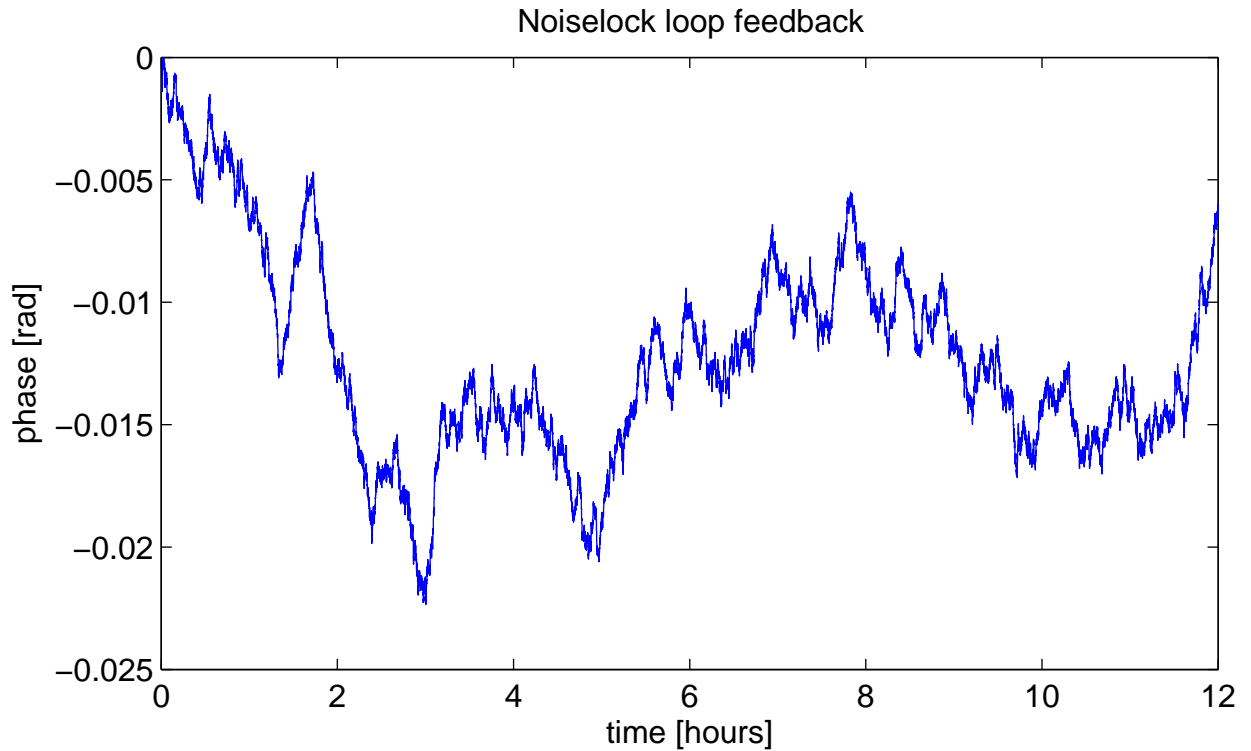

Figure 8: Example of drift of squeezer demodulation phase over the course of 12 hours.
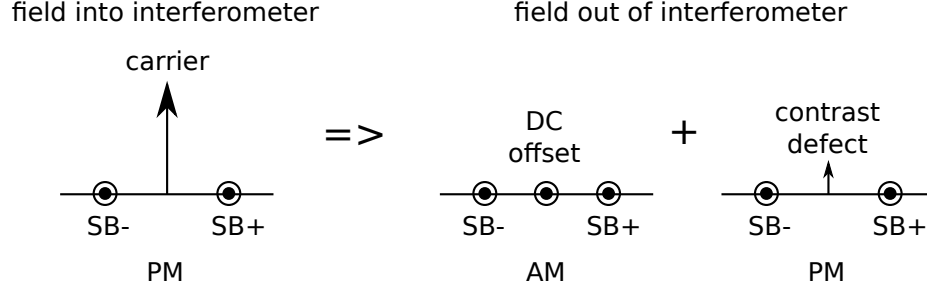
Figure 9: The RF sidebands (SB+ and SB-) are generated via phase modulation of the carrier field. The Michelson interferometer rotates the differential carrier field by 90°, but leaves all other fields the same, including the RF sidebands and the contrast defect. The result is that at the output port, the RF sidebands are amplitude modulation (AM) of the dark fringe offset, yet continue to be phase modulation (PM) of the contrast defect.

5.3   RF frequencies

This section is based on work from LIGO T0900325 and evaluates the role of the RF sidebands in generating phase jitter of the interferometer output field. Understanding the phase noise contribution from the RF sidebands is important both because the contribution can be large and because the squeezing ellipse orientation cannot follow at these frequencies. Phase noise due to the RF sidebands may, however, be reduced, as will be discussed shortly.

The dominant fields at the interferometer output port are those from the dark fringe offset, the contrast defect, and the RF sidebands. The dark fringe offset is the local oscillator for the gravitational-wave sidebands in a DC readout configuration and is generated by holding the Michelson arms slightly off of the dark fringe at the anti-symmetric port. The contrast defect is light that makes it to the anti-symmetric port due to asymmetry in the reflectivity of each Michelson arm. The RF sidebands are ideally filtered by the OMC, but due to limited finesse, some percentage is transmitted.

One of two effects of the RF sidebands on phase jitter comes from the fact that the Michelson interferometer rotates the differential carrier field by 90°, but leaves all other fields the same (including the RF sidebands and the contrast defect). The result is that at the output port, as shown in Figure 9, the RF sidebands are amplitude modulation (AM) of the dark fringe offset, yet continue to be phase modulation (PM) of the contrast defect.

Because the squeezing quadrature is determined by the sum of the fields at the interferometer output, both AM of the dark fringe offset and PM of the contrast defect affect the angle that the squeezing ellipse orientation must be matched to. Figure 10 shows phasors depicting these two situations. Should the ratio of dark fringe offset to contrast defect amplitude be large, these effects are reduced.

The second effect of the RF sidebands on phase jitter arises when the upper and lower sidebands are unequal in amplitude. Rather than produce pure AM on the DFO and PM on the CD, there is some component of PM on the DFO and AM on the CD.
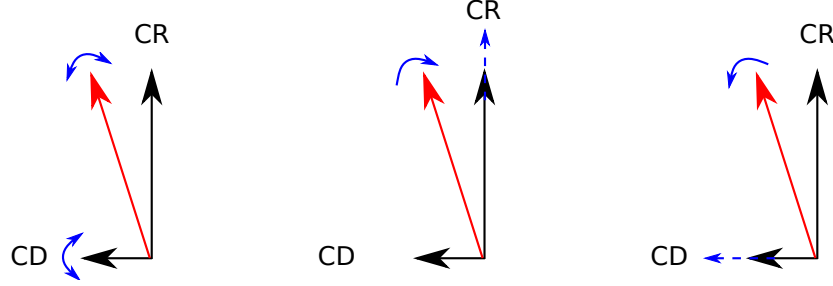
Figure 10: Examples of how jitter of the squeezing quadrature is generated. replace!

In summary, changes in the interferometer output phase at RF frequencies are created in four ways:

- phase noise of the contrast defect

- amplitude noise of the dark fringe offset

- phase noise of the dark fringe offset due to unequal RF sideband amplitudes

- amplitude noise of the contrast defect due to unequal RF sideband amplitudes (true?)

and may be expressed mathematically as in Eq. 90 from T0900325:

$$\Gamma_{\mathrm{rms}} = \sqrt{\frac{P_{\mathrm{SB}}}{P_{\mathrm{CR}}} \left(\frac{1}{\eta} + \epsilon^2 \frac{\eta - 1}{\eta} \right)} \tag{4}$$

All powers in this equation are for those transmitted through the OMC, and the variables η and ϵ are defined as follows:

$$\eta = \frac{P_{\mathrm{CR}}}{P_{\mathrm{CD}}} \tag{5}$$

$$\epsilon = \frac{1}{2} \frac{P_{\mathrm{SB+}} - P_{\mathrm{SB-}}}{P_{\mathrm{SB+}} + P_{\mathrm{SB-}}} \tag{6}$$

The sideband imbalance is quantified by ϵ and a sample measurement of the imbalance is shown in Figure 11a. Currently, $\epsilon = 0.06$. The contrast defect, commonly quoted as $1/\eta$, can be measured by comparing the power transmitted through the OMC with and without the dark fringe offset. It accounts for approximately 5% of the power at the output port, as seen in Figure 11b.

Figure 12 shows the dependence of phase noise on contrast defect for our current sideband imbalance. This uses $P_{CR} = 1.6$ and $P_{MI\_SB+} = 0.08T_{MI}$ (for the 4.4× sideband amplitude reduction). We estimate the signal recycling cavity sideband amplitude as $P_{SR\_SB+} = 0.02T_{SC}$. Note T_{MI} and T_{SR} are calculated in Table 6. We explored the effect of these factors on observed squeezing by changing the rms phase noise up to a factor of 4.4 by reducing the sideband amplitude. We also tried increasing the dark fringe offset.
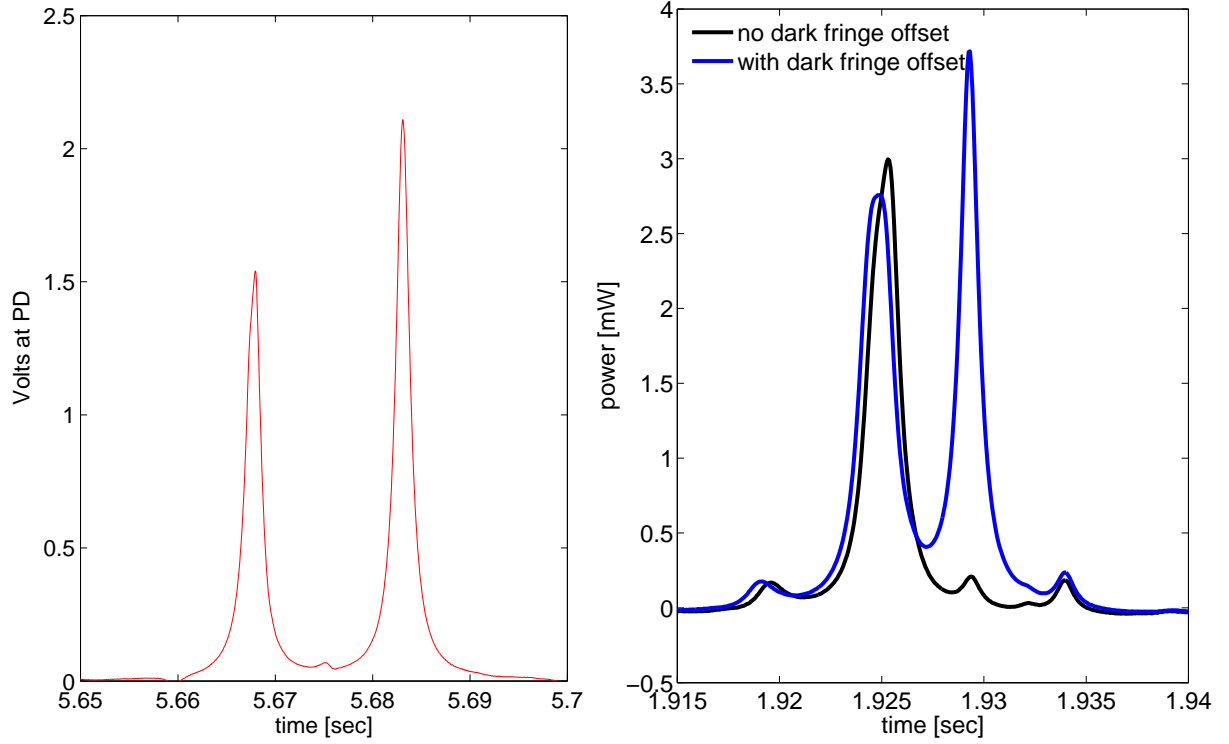
Figure 11: Mode scan of the output port. The left-hand plot shows the Michelson RF sideband imbalance. A higher-order carrier mode sits on top of the lower sideband, so this figure is created by subtracting the carrier content. The imbalance is $\epsilon = 0.06$. The right-hand plot shows the ratio of contrast defect to carrier power for our typical dark fringe offset. The ratio is about 0.05. The sideband amplitude is reduced by a factor of 4.4 from fall 2011 and is the new standard.
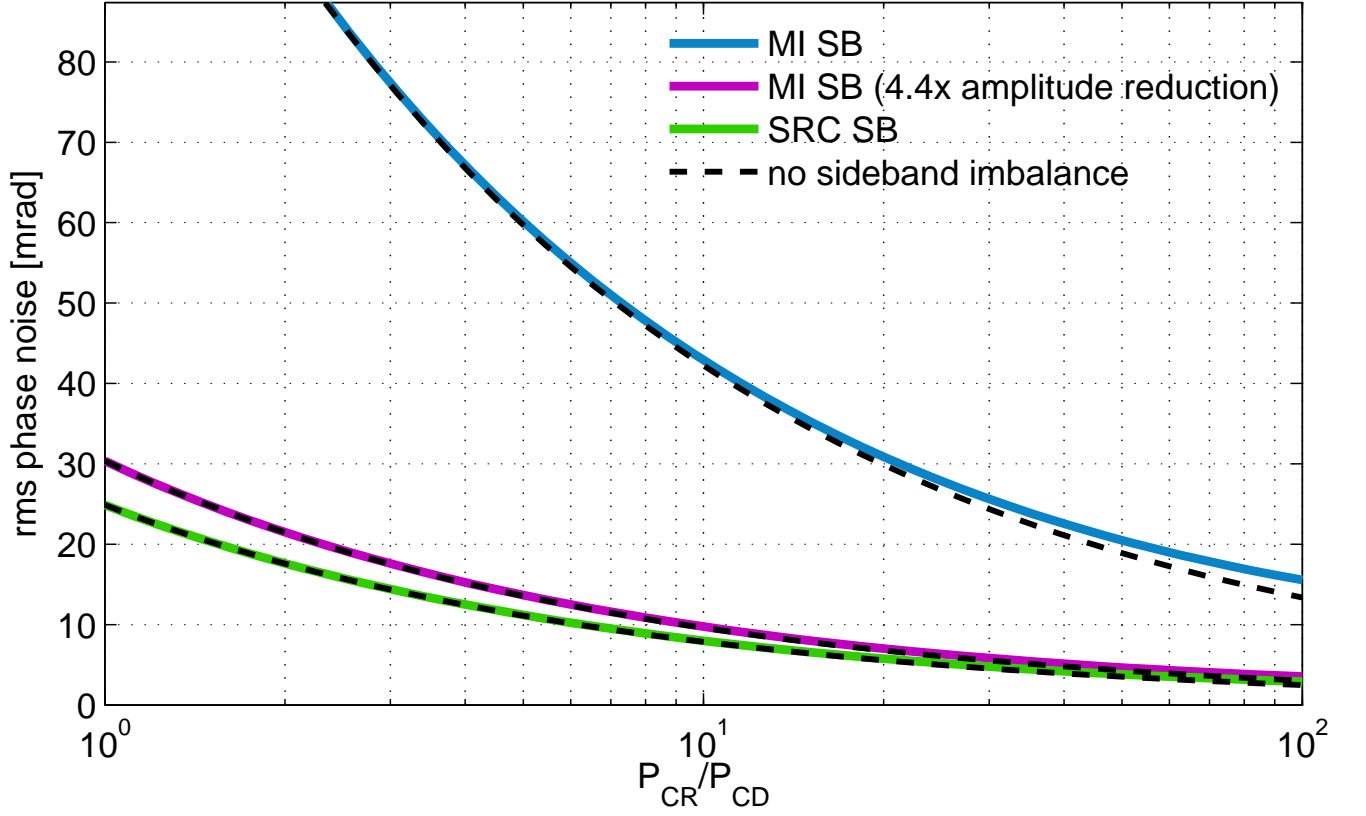
Figure 12: RMS phase noise as a function of the ratio of DC offset light to contrast defect light in the OMC transmitted beam. The typical operating point for GEO is $P_{CR}/P_{CD} = 20$, which corresponds to an RMS phase noise for the Michelson sidebands of 6.7 mrad and 5.5 mrad for the SRC sidebands. The quadrature sum is 8.7 mrad.

Table 4: Measured and calculated phase noises. The quadrature sum is 10 mrad rms.

source	rms phase [mrad]
error point	5
14.9 MHz sidebands	6.7
9 MHz sidebands	5.5

5.4   Higher order modes

Role?

5.5   Total known phase noise

Taking the measured and anticipated rms phase noises at different frequencies and adding them incoherently, we find that we have a total known phase noise of 10 mrad rms. The summary of phase noises is shown in Table 4.

5.5.1   Measuring total phase noise

We currently do not have information about the rms phase noise between audio and RF frequencies. We can indirectly determine what it is by measuring the total phase noise via its affect on the squeezing level. We can measure the total rms phase noise by mapping out the curve of Figure 3. However, this will be difficult if the total phase noise happens to be very small (< 10 mrad) because then the effect of phase noise is only measurable at very high pump powers. At the moment, we are limited to at most only approx. 25 mW pump power and we know of only approx. 10 mrad phase noise. A method of putting an upper limit on the total phase noise is to purposefully increase it by a known amount (i.e. keep amplitude of MI RF sidebands at nominal locking level) and measure the squeezing versus pump power curve. This will also provide a way of calibrating the CDS counts of pump power into mW.

6   Expected observed squeezing

Based on our measurements of the optical losses and phase noise, we can predict the best possible achieveable squeezing level with the interferometer output. With a green pump power of about 17 mW such that the injected squeezing level is 8 dB and with 37% losses, the best squeezing possible is 3.2 dB. Phase noise of 10 mrad has a negligible effect. As of early March, we measured 2.9 dB, leaving a 0.3 dB gap, which in fact is explained by other contributing noise sources at high frequencies such as dark noise and laser amplitude noise. Figure 13 shows an example of these other noise levels as of mid-April. This full accounting
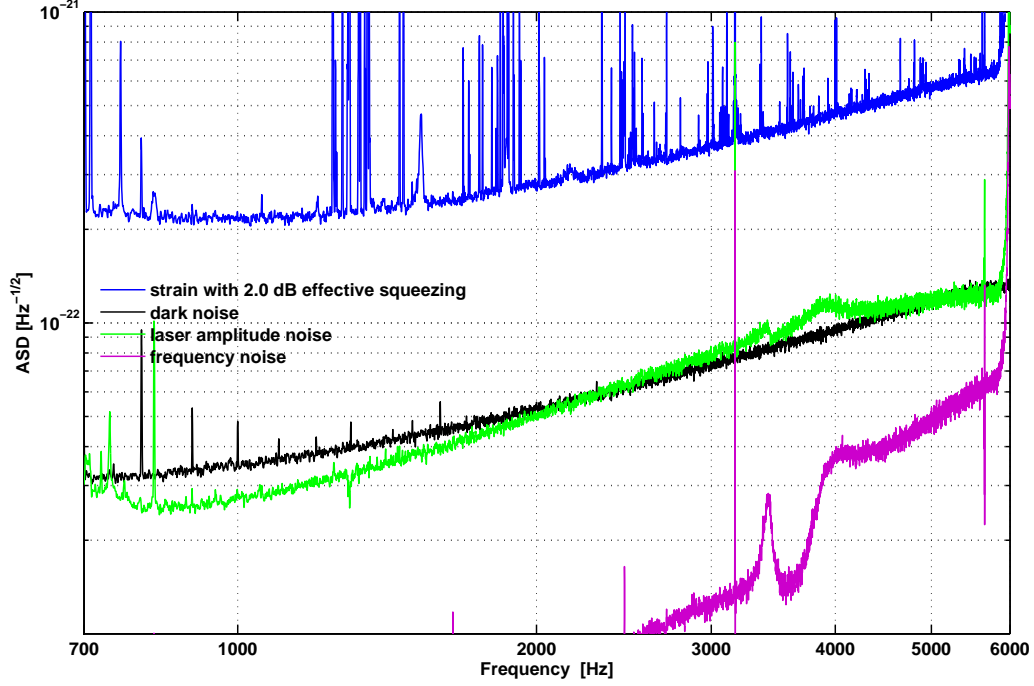
Figure 13: High frequency noises that result in a lower effective squeezing of strain than is actually achieved. In this example, shot noise is actually reduced by 2.4 dB due to squeezing, but the other noise sources, when added in quadrature with shot noise, reduce the effective squeezing to 2.0 dB. In this example, laser amplitude noise is abnormally high.

of observed squeezing is not always realized, however. Since mid-April, for example, there remains a gap.

7   Ideas for improvements

1. better OMC

2. 2 PDs for an on-board homodyne detector (?)

3. 2nd OMC

8   Acknowledgements

Table 5: Optical losses of squeezed beam.

component	power loss	6-month goal
squeezer path Faraday	3.3%	1.5%
output port Faraday	3.3% × 2	1.5% × 2
BDO1 transmission	1% × 2	1% × 2
SR cavity (when locked)	1%	1%
OMC mode-matching loss	6%	2%
squeezer mode-matching loss	2%	2%
OMC AR coating loss	1%	0.1%
OMC internal losses	14%	5%
OMC trans PD detection loss	9%	3%

Table 6: OMC parameters. Many numbers come from p.12 of the GEO-HF logbook.

quantity	symbol	value	units
Finesse	F	160	
round trip length	L	0.658	m
g-factor	g	0.735	
waist size	ω_0	450	µm
free spectral range	FSR	455.6	MHz
Michelson sideband frequency	f_{MI}	14.90	MHz
SRC sideband frequency	f_{SR}	9.18	MHz
Michelson sideband power transmission	T_{MI}	1.01	%
SRC sideband power transmission	T_{SR}	2.71	%

9   Appendix–OMC

Table 6 summarizes the current output mode cleaner (OMC) design parameters. Note that the sideband transmission numbers (T_{MI} and T_{SR}) should be doubled in practice to account for the existence of both upper and lower sidebands.